BAU Journal - Science and Technology

Volume 4 | Issue 2
ISSN: 2959-331X

Article 1

June 2023

LOCALIZED SURFACE PLASMON RESONANCE OF PALLADIUM PARALLELEPIPED NANOPARTICLES

Salem Marhaba
Department of Physics, Faculty of Science, Beirut Arab University, Lebanon, s.marhaba@bau.edu.lb

Nourhan El Kawni
Department of Physics, Faculty of Science, Beirut Arab University, Lebanon, kawninourhan@gmail.com

Recommended Citation

Marhaba, Salem and El Kawni, Nourhan (2023) "LOCALIZED SURFACE PLASMON RESONANCE OF PALLADIUM PARALLELEPIPED NANOPARTICLES," *BAU Journal - Science and Technology*: Vol. 4: Iss. 2, Article 1.
DOI: https://doi.org/10.54729/2959-331X.1093

1. INTRODUCTION

The interaction of light with the electrons of atoms and molecules found inside matter has been an important field for study for many scientists throughout the years. R.M. Wood (Wood, R. 1902) has realized that when incident polarized light strikes a metal diffraction grating, a pattern of bizarre dim and light bands showed up within the reflected light. Even though, R.M. Wood had some sort of research about how metals and electromagnetic waves interact, he wasn't able to give a clear interpretation of this situation. Hypothetical investigation embraced by Fano (Fano, U. 1941) driven to the conclusion that the phenomenon found on the surface of the material were related with surface wave. Otto (Otto A. 1968) stated that waves which are situated on the surface can be energized by taking an advantage of the formulation of reflection. Kretschmann and Raether (Kretschmann, E.; Raether, H. 1968) had the same outcomes by a various arrangement of the attenuated total reflection method. After this amount of work by these scientists, the interest of the whole science community for confined electrons in a surface has increased greatly, especially for studying them on metal surfaces. Liedberg and Nylander (Liedberg *et al.* 1983) marked a turning point in the particle's surface research in 1983.

When the size of a metal-based material is decreased to the nanometers range, the optical properties are altered by the appearance by the phenomenon Localized Surface Plasmon Resonance (LSPR) and it's seen that the behavior and interaction becomes highly different when comparing it to bulk metal-based materials (Billaud *et. al.* 2008, Petryayeva *et al.* 2011). LSPR is a collective oscillation of conduction electrons which are excited by the electromagnetic field of light in a metallic nanoparticle. The electrons oscillations actuate an electric field around the nanoparticle that can be much bigger than the incident light one. Subsequently, LSPR can be utilized in a wide extend of areas in biomedical fields (Kang *et al.* 2018 and Chatterjee *et al.* 2014), environment security (Deplanche *et al.* 2014), detecting and data innovation applications (Saldan *et al.* 2015).

Palladium is a valuable element that is commonly used in organic catalysis reactions (Maiti *et al.* 2012). Adams et al. (Adams *et al*. 2014) investigated the antibacterial activity of palladium (Pd) nanoparticles. The Pd nanoparticles showed high growth prevention against Staphylococcus aureus which is a gram-positive bacteria that cause a wide variety of clinical diseases, as compared to another bacterial species. The importance of Pd nanoparticles is valuable against the anti-bacterial agent, particularly for gram-positive microbes. Sachse et al. (Sachse *et al.* 2013) mentioned that when Pd nanoparticles was assembled over nanomaterials made up of mesoporous silica, it showed higher cytotoxic activities against human cancer cell lines. Pd-based nanomaterials and Pd@M (M=Ag, Au, Pt or SiO_2) nanocomposites exhibit strong absorption in the near-infrared region, excellent photothermal stability, and good biocompatibility as mentioned before. Taking into consideration these important characteristics of Pd-based nanomaterials it has become a leading candidate as cancer imaging agents and therapeutic agents. Their synthesis and properties have been discussed in several review papers (Chen A. *et al.* 2015, Chen M. *et al.* 2012 and Chen X. *et al.* 2017). Pd nanoparticles can be used in photothermal therapy (PTT), which is a new way to treat cancer, in which cancer cells are ablated by the heat generated from an optically absorbing agents upon laser irradiation, exhibiting minimal side effects, high specificity and controllability (Liu Y. *et al.* 2020). While comparing the results of Au nanomaterials to Pd nanomaterials the last had an advantage in photothermal stability and photothermal conversion efficiency over the first.

In this paper, we present theoretical analysis of the size and shape effects on LSPR of a single palladium nanoparticle. It will be studied by resolving Maxwell equations using finite element method (FEM) in the frame of COMSOL Multiphysics software. Two cases of a parallelepiped Pd nanoparticle are considered. The first case studies the size effect on LSPR upon fixing the height and varying both length and width within a range of 50 to 100 nm. However, the second case studies the shape effect on the LSPR of a parallelepiped Pd nanoparticle. To do so, we intended to fix the height, length, and width at 50 nm, 100 nm, and 50 nm respectively and to change the corners' radius in a range of 0 to 15 nm. The extinction cross-section spectra of these different size and shape of nanoparticles are calculated for different electromagnetic wave polarization. The calculations are performed over a broad spectral range from 200 to 900 nm. The surrounding medium for various palladium nanoparticles is the air.

2. MIE THEORY AND FINITE ELEMENT METHOD SIMULATIONS:

An electromagnetic plane wave is incident to a spherical nanoparticle of diameter D, dielectric permittivity ε and magnetic permeability μ embedded in transparent medium ε_m. The electromagnetic plane wave of wavelength λ interacts with the free electrons found in the conduction band of the nanoparticle (Lermé *et al*. 2008, Baida *et al*. 2009). To obtain the far-field optical response of nanoparticle, we should determine the solution of Helmholtz equations (Marhaba, 2018):

$$\begin{cases} \vec{\nabla}^2 \vec{E} + k^2 \vec{E} = \vec{0} \\ \vec{\nabla}^2 \vec{H} + k^2 \vec{H} = \vec{0} \end{cases}, \qquad (2.1)$$

where, the electromagnetic field $\{\vec{E}, \vec{H}\}$ is described by Maxwell's (Kreibig and Vollmer, 2013) and $k^2 = \varepsilon\mu\,\omega^2$.

In quasi-static approximation the size of the particle is much smaller the wavelength of the electromagnetic wave ($D = 2R \ll \lambda$). The phase of the electromagnetic field, which is oscillating harmonically, is constant over the whole volume. This will allow us to calculate the spatial field distribution electrostatically. The polarizability α is given by

$$\alpha = 4\pi R^3 \frac{\varepsilon - \varepsilon_m}{\varepsilon + 2\varepsilon_m} \qquad (2.2)$$

The resonance condition is obtained when

$$Re[\varepsilon(\omega)] = -2\varepsilon_m \qquad (2.3)$$

which is known as Fröhlich condition (Kreibig and Vollmer, 2013). Equation (2.3) tells that the resonance frequency depends on the dielectric environment and the resonance red shifts as ε_m is increased. The scattering and absorption cross-sections can be expressed as:

$$\sigma_{sca} = \frac{k^4}{6\pi}|\alpha|^2 = \frac{8\pi}{3}k^4R^6\left|\frac{\varepsilon - \varepsilon_m}{\varepsilon + 2\varepsilon_m}\right|^2 \qquad (2.4)$$

$$\sigma_{abs} = kIm[\alpha] = 4\pi kR^3 Im\left|\frac{\varepsilon - \varepsilon_m}{\varepsilon + 2\varepsilon_m}\right| \qquad (2.5)$$

For very small particles when $R \ll \lambda$, the efficiency of absorption, which is proportional to R^3, dominates over the scattering efficiency, which is proportional to with R^6. Enhancement of the absorption and scattering cross sections could occur when Fröhlich condition given in equation (2.3) is met, and that's actually seen in equations (2.4 and 2.5). The expression of the extinction cross section for a spherical geometry of volume *V* and dielectric function $\varepsilon = \varepsilon_1 + i\varepsilon_2$, which is given by $\sigma_{ext} = \sigma_{sca} + \sigma_{abs}$ within the quasi-static limit is given by:

$$\sigma_{ext} = 9\frac{\omega}{c}\varepsilon_m^{3/2}V\frac{\varepsilon_2}{[\varepsilon_1 + 2\varepsilon_m]^2 + \varepsilon_2^2} \qquad (2.6)$$

The quasi-static approximation considers the surface charges as a dipole, but when the size of nanoparticle increases the distribution of charges may have multipolar contribution of higher orders and we consider these now. Mie theory gives an exact general calculation of the optical response for a spherical particle of any diameter having a size range where kR is no longer limited. Let us define M which gives the ratio between the dielectric constant of the nanoparticle and that of the medium surrounding it, and *x* the dimensionless size parameter (Marhaba, 2018):

$$M^2 = \frac{\varepsilon}{\varepsilon_m} = \left(\frac{n}{n_m}\right)^2 \quad and, \quad x = kR = \frac{2\pi n_m R}{\lambda} \qquad (2.7)$$

Extinction, scattering and absorption cross sections can be expressed as

$$\sigma_{ext} = \frac{2\pi}{k^2}\sum_{n=1}^{\infty}(2n+1)Re\{a_n + b_n\} \qquad (2.8)$$

$$\sigma_{sca} = \frac{2\pi}{k^2}\sum_{n=1}^{\infty}(2n+1)Re\{|a_n|^2 + |b_n|^2\} \qquad (2.9)$$

$$\sigma_{abs} = \sigma_{ext} - \sigma_{sca} \qquad (2.10)$$

For a nanoparticle of diameter D. The coefficients a_n and b_n are defined by:

$$\begin{cases} a_n = \frac{M\varphi_n(Mx)\varphi_n'(x) - \varphi_n(x)\varphi_n'(Mx)}{M\varphi_n(Mx)\zeta_n'(x) - \xi_n(x)\varphi_n'(Mx)} \\ b_n = \frac{\varphi_n(Mx)\varphi_n'(x) - M\varphi_n(x)\varphi_n'(Mx)}{\varphi_n(Mx)\zeta_n'(x) - M\xi_n(x)\varphi_n'(Mx)} \end{cases} \qquad (2.11)$$

where, φ_n and ξ_n are the Riccati-Bessel functions of order n, n is the order of the multipole expansion.

In the case of non-spherical nanoparticles (cube, pyramids, star…) (Amendola *et al.* 2010, Nehl *et al.* 2006), organized nanoparticles (dimer, trimer, chain, …) (Marhaba *et al.* 2009, Marhaba and El Samad. 2020, Marhaba and El Samad. 2021) or arrays of nanoparticles (Marhaba, 2015) the solution of Maxwell's equations are determined numerically. Extinction cross section spectra of nanoparticles of arbitrary geometries and arrangements (El Samad and Marhaba. 2022) can be calculated using different methods such as finite difference time domain (FDTD) (Sadiku, 2000) discrete dipole approximation (DDA) (Yurkina *et al.* 2007) and finite element method (FEM) (Pradhan *et al.* 2018). In this paper, FEM is applied to compute numerically the electric field and the optical response of Pd nanoparticles using COMSOL Software for Multiphysics Simulation 5.2a (Dickinson *et. al.* 2014).

3. COMSOL REQUIREMENTS:

COMSOL needs some basic information as parameters, geometry, materials and meshes to design the nanostructure and execute the simulation. We start with a new 3D model. The interface chosen is Radio Frequency, and then the Electromagnetic Waves, Frequency Domain (emw).

To run the program, we should first insert several components, shown below:

3.1 Parameters:

The parameters are the constants that our program will be built on, such as the incident electric field amplitude E_0, the geometry dimensions (height, width and length) of the parallelepiped, wavelength range of the incident electromagnetic wave incident (λ), incident light intensity (S_{in}), radius (r_{pml}) and thickness (t_{pml}) of perfectly matched layer (PML).

Table 1: Parameters

Name	Expression	Value	Description
E_0	1[V/m]	1 V/m	Electromagnetic Field
height	50	50	Height of the parallelepiped
width	50	50	Width of the parallelepiped
length	50	50	Length of the parallelepiped
lambda	200	200	Initial Wavelength
lambda_min	200	200	Minimum Wavelength
lambda_max	900	900	Maximum Wavelength
lambda_step	5	5	Wavelength Step
S_in	$E_0^2/2Z_0\_const$	0.0013272 W/m^2	Scaling Factor
r_pml	500	500	PML Radius
t_pml	150	150	PML Thickness

3.2 Geometry, Material and Meshes:

We have two geometries to obtain the desired design and calculate its optical response: the nanoparticle (geometry, size, shape and material) and the spherical perfectly matched layer (PML) as shown in Figures 1(a) and 1(b). In our case, we construct palladium parallelepiped nanoparticle embedded in air. Concerning the material, the dielectric constants of palladium are extracted from (Johnson and Christy, 1972). We should mention that the physical domain includes the nanoparticle geometry and the surrounding medium which the light will be incident on. We apply a perfectly matched layer (PML) to absorb and prevent reflection of the incident fields as shown in Fig. 1 (b). An electromagnetic plan wave strikes the surface of the palladium parallelepiped nanoparticle embedded in air. To calculate the solution of Maxwell's equation of electric field presented in equation (2.1) using FEM, we should discretize the geometries into finite elements. A free triangular mesh was chosen for both Pd nanoparticle and PML surface. Whereas, the thickness of the PML is meshed by using free tetrahedral shape (Figure 1.c). COMSOL software comes up with a ready-to-use perfectly matched layer button (Grand, 2019), in which you can use it then choose your preferred geometry. Usually, tetrahedron shape is used for the thickness of the perfectly matched layer domain (Gracia *et al.* 2008).

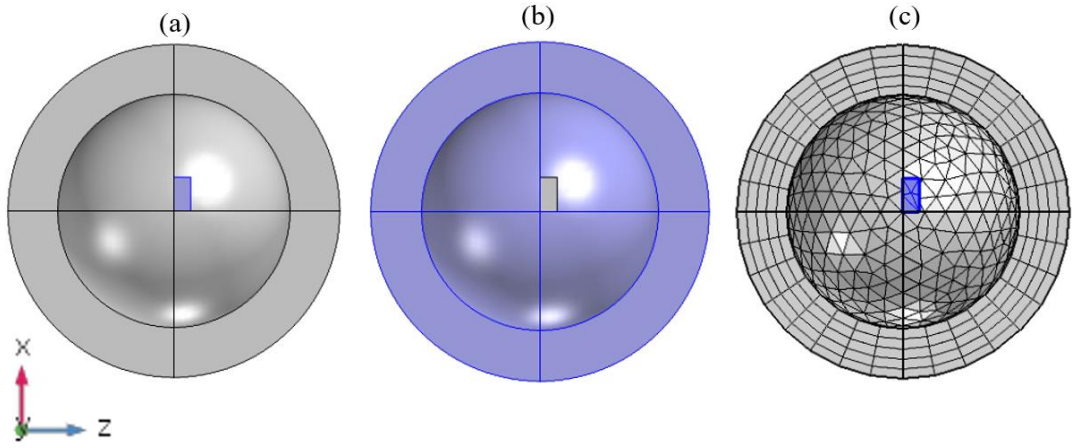

Fig.1: (a) Pd parallelepiped (b) Perfectly matched layer PML (c) boundary layers meshes

3.3 Definitions:

The scattering and absorption cross-sections are computed by evaluating the surface and volume integrals according to the following equations:

$$\sigma_{sc} = \frac{1}{I_0} \iint (\vec{n}.\vec{S}_{sc}) dS, \qquad (2.12)$$

and

$$\sigma_{abs} = \frac{1}{I_0} \iiint Q dV, \qquad (2.13)$$

where I_0 is the incident light intensity, $\vec{n}$ is the normal vector pointing outward from the considered surface element, $\vec{S}_{sc}$ is the scattered Poynting vector and Q is the power loss density inside the nanoparticle. In COMSOL, the expression intop_surf(nrelPoav)/S_in) is equivalent to equation (2.12) and the expression intop_vol(emw.Qh)/S_in) is equivalent to equation (2.13) as shown in Table 2.

Table 2: Definitions

Name	Expression	Unit	Description
sigma_sc	intop_surf(nrelPoav)/S_in)	m^2	Scattering Cross Section
sigma_abs	intop_vol(emw.Qh)/S_in)	m^2	Absorption Cross Section
sigma_ext	sigma_sc + sigma_abs	m^2	Extinction Cross Section

4. RESULTS AND DISCUSSIONS:

The extinction cross sections $\sigma_{ext}\ (nm^2)$ as function of the wavelength $\lambda\,(nm)$ are represented graphically to show the shape and size effect on the LSPR of a parallelepiped Pd nanoparticle. Two different cases have been considered: varying the width and length of a parallelepiped nanoparticle while fixing its height (size effect) and rounding the corners of a parallelepiped at different radii (shape effect). The surrounding medium for the palladium nanoparticle is taken air ($\varepsilon_m = 1$) for all cases. Figure 2 illustrates the palladium parallelepiped nanoparticle with variable length and width and constant height of value 50nm.

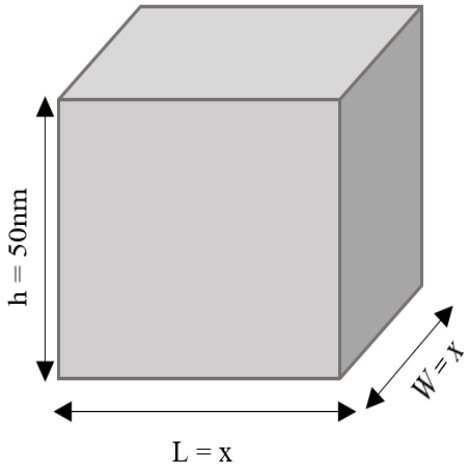

Fig.2: Dimensions representation of the parallelepiped Pd nanoparticle

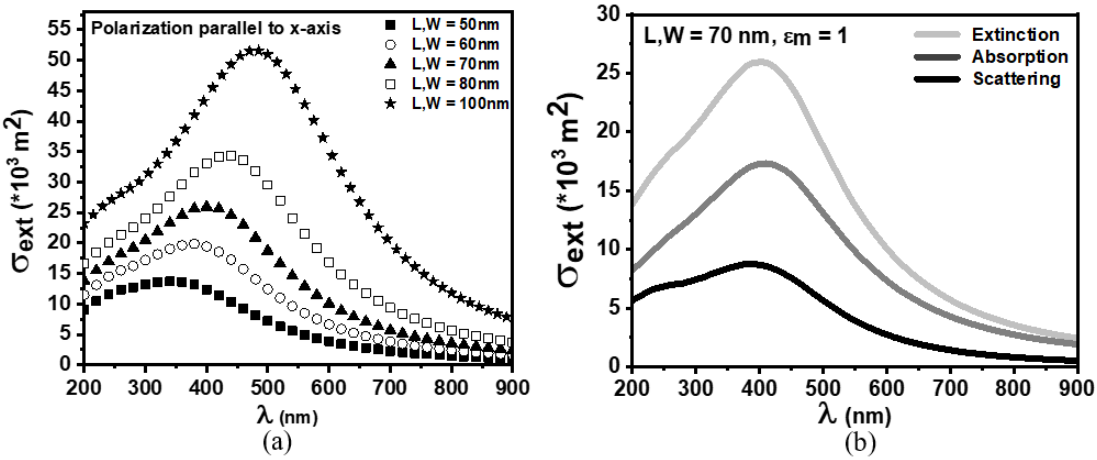

Fig.3: (a) Extinction cross sections spectra upon varying the length and width from 50 to 100 nm calculated using FEM of Pd parallelepiped for polarization parallel to x axis. (b) Extinction, absorption and scattering cross section spectra of Pd nanoparticle of length and width 70 nm placed in air and calculated by FEM.

Figures 3 (a) shows the σ_{ext} spectra for palladium nanoparticle having the shape of parallelepiped of the length and width in the range 50 to 100nm for polarization along x-axis as function of wavelength. We can conclude that the peak resonance shifts to longer wavelengths (red shift) as the nanoparticle length and width increase. Moreover, the intensity of the extinction cross section is increasing as a result of the increase of the material quantity (Table 3).

Table 3: Peak wavelength and magnitude of extinction cross section of palladium parallelepiped nanoparticles of various lengths and widths in the surrounding of air medium

Length and Width of the nanoparticle (nm)	Peak Resonance λ_{max} (nm)	Extinction Cross Section (nm^2)
50	335	13749.67276
60	380	19894.3409
70	400	25954.17284
80	435	34370.75005
100	480	51649.06265

The increase of the size induces a broadening and red shifting (Fig. 3 (a)) of the resonance due to the increasing influence of the multipolar terms. Regarding the width of LSPR, multiple parameters will play on its evolution with the size of the particle. For a single Pd nanoparticle, the width of the resonance reflects the lifetime of the collective excitation. The width is inversely proportional to the lifetime so as the lifetime gets shorter the width of the nanoparticle increases. All processes of collisions of the electrons (electron-electron, electron-phonon ...) will limit the lifetime of the plasmon resonance contributing to the dissipation of energy, which decreases the spectral amplitude and broadens the spectral width of LSPR. For more understanding the extinction cross section behavior, we calculate the scattering and absorption cross sections spectra of single parallelepiped Pd nanoparticle for length and width of 70 nm and height of 50 nm as shown in Fig. 3 (b). As we saw in section 3, the extinction cross section of metal nanoparticle is the sum of absorption and scattering cross-sections (Bohren *et al.* 1983 and Kreibig *et al.* 1995). It is obvious that the extinction is strongly dominated by the absorption cross-section. The extinction spectrum shows a spectral peak which corresponds to the LSPR around 400 nm.

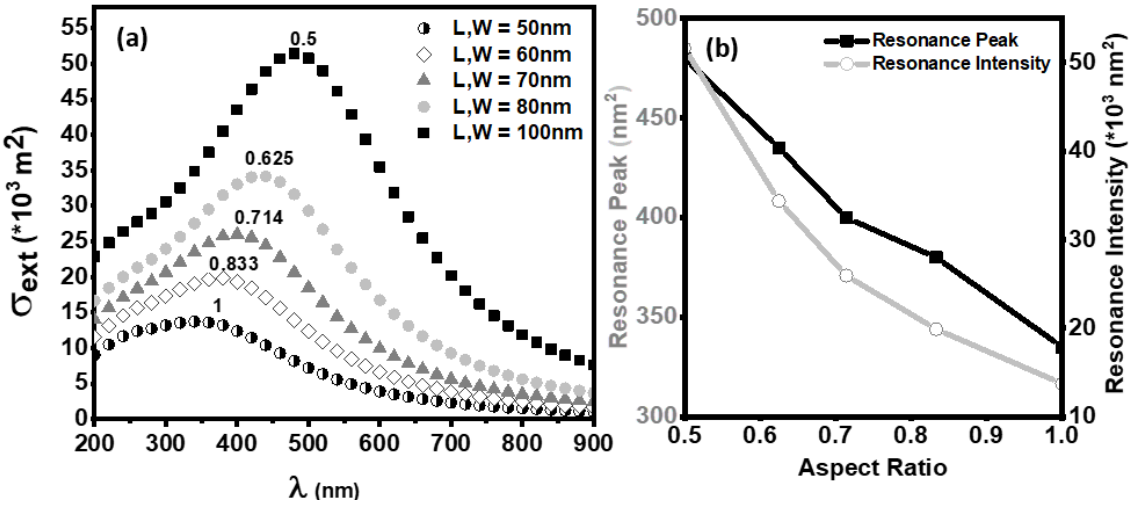

Fig.4: (a) Calculated extinction spectra for Pd parallelepiped according to case 2, polarization along x-axis, with different aspect ratio indicated in the figure. (b) Resonant position and intensity of the SP as a function of the parallelepiped aspect ratio.

Fig. 4 (a) shows the aspect ratio, which is the ratio of height to width, of the parallelepiped. We notice that the peak resonance is having a red shift (larger wavelengths of range 330 to 480nm). Moreover, the extinction cross section intensity increases with the increase of length and width.

As the aspect ratio increases, the peak resonance and extinction cross section decrease (see Fig. 4 (b)). The reason behind that is that as the width of the parallelepiped nanoparticle increases, the charge accumulation on the surface of the nanoparticle increases too, leading to high extinction intensities. The restoring force is proportional to this charge accumulation, and therefore, for electrons oscillating along the height surface we should expect smaller forces and consequently smaller resonance frequencies thus higher resonance wavelengths. The resonance condition is met when $\varepsilon_1 = -2\varepsilon_m$, which occurred in the near ultraviolet range for length and width up to 70nm. The peak changes to the visible range once the length and width moved from 80nm to 100nm.

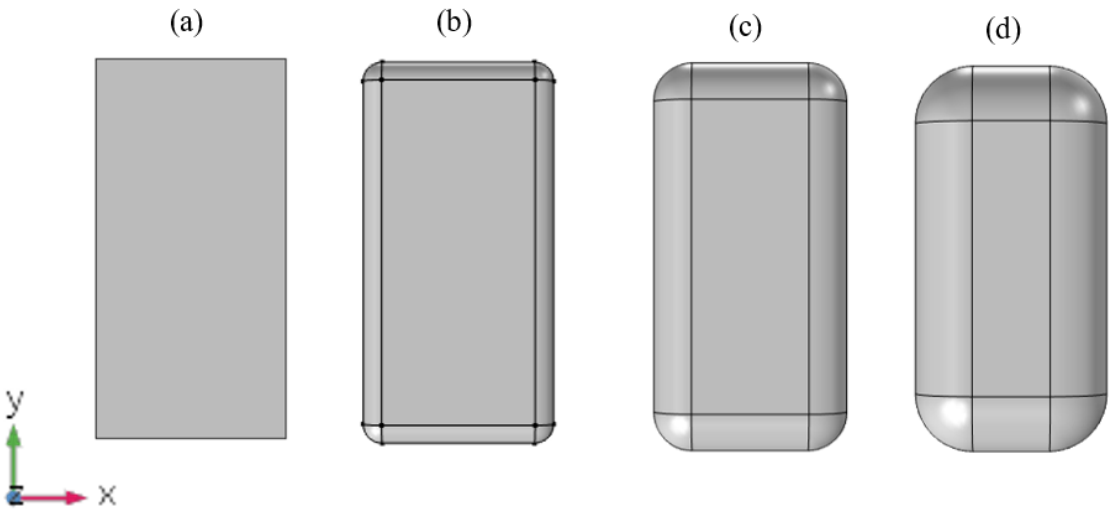

Fig.5: Pd parallelepiped nanoparticle with corners of radius (a) 0 nm (b) 5 nm (c) 10 nm, (d) 15 nm.

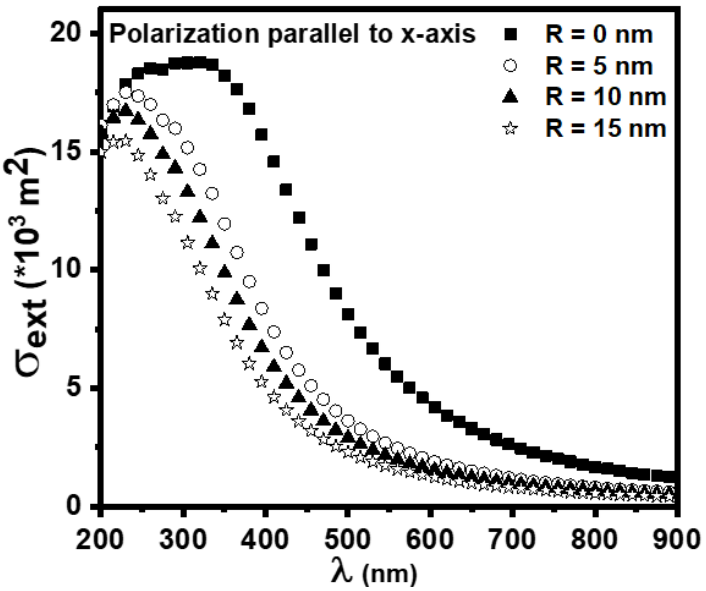

Fig.6: Extinction cross sections spectra upon varying the corner's radius from 0 to 15 nm calculated using FEM of Pd parallelepiped for polarization parallel to x axis.

Figure 5 illustrates the palladium parallelepiped nanoparticle with fixed length (50nm), width (100nm) and height (50nm) while rounding the corner, which is the second case. Extinction cross sections spectra upon varying the corner's radius from 0 to 15 nm are calculated using FEM of Pd parallelepiped for polarization parallel to x axis (Fig.6). When $R = 0\ nm$ there was a flat peak resonance, by increasing the corner's radius from 5 to 15nm a sharper peak is obtained. The extinction spectrum shows a spectral peak which corresponds to the LSPR between 225 and 265 nm (near ultraviolet region) when the nanoparticle is placed in air (ε_m = 1). Moreover, the intensity of extinction cross section decreased with the increase of the corners' radius (Table 4). This is a

result of the cut-off of the nanoparticle volume which clearly affects the localized surface plasmon resonance.

Table 4: Peak wavelength and magnitude of extinction cross section of palladium parallelepiped nanoparticles of different corner radii (polarization along x-axis)

Corner radius of the nanoparticle (nm)	Peak λ_{max} (nm)	Extinction Cross Section
0	320	18774.27033
5	235	17537.52967
10	225	16733.31783
15	225	15553.09393

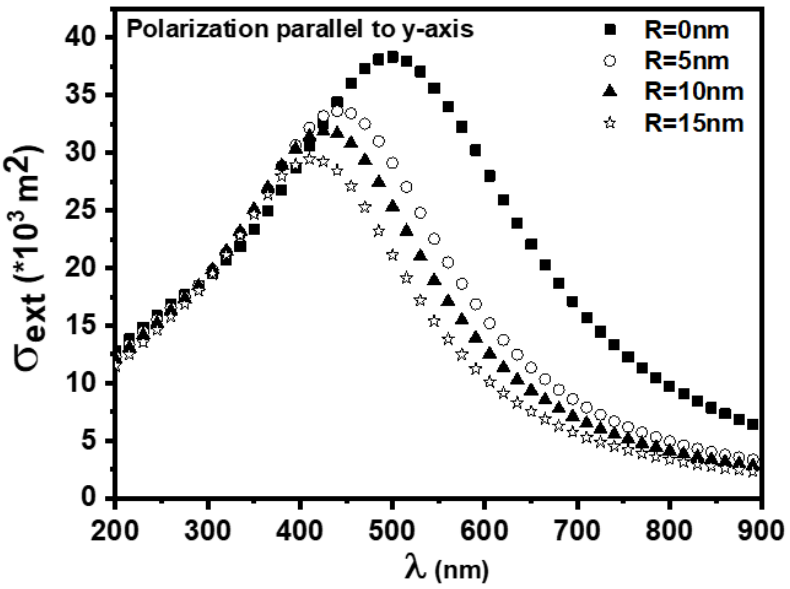

Fig.7: Extinction cross sections spectra upon varying the corner's radius from 0 to 15 nm calculated using FEM of Pd parallelepiped for polarization parallel to y-axis.

Figure 7 shows the variation of extinction cross section as function of the wavelength within the change of the corner shape when the polarization is parallel to y-axis. As shown in Figure 7, the spectral peak position of wavelength is blue shifted as the radius on the corners of the parallelepiped nanoparticle is increased (Table 5). This blue shift is due to the decrease of the surface size of the nanoparticle due to the round shape corner. The results showed that when polarization was along x-axis, which means that it was perpendicular to the nanoparticle (transversal direction), we had a resonant wavelength of 225nm for a corner radius of 15nm. However, when the polarization of the electromagnetic wave changed into the y-direction, we got lower energy of the oscillating electrons on its surface thus higher wavelength resonance peak of 415nm in the same case. This verifies that when the electromagnetic wave is parallel to x axis of parallelepiped having dimensions (50 nm, 100nm, 50 nm) we get lower wavelength resonance peaks. When the polarization of light is parallel to y axis, we have higher peaks due to larger numbers of oscillating electrons on the surface.

Table 5: Peak wavelength, magnitude and width of extinction cross section of palladium parallelepiped nanoparticles of corner fillet radii in the surrounding air medium (incident light polarization along y-axis)

Corner radius of the nanoparticle (nm)	Peak λ_{max} (nm)	Extinction Cross Section	Width (nm)
0	500	38317.74302	369.61067
5	445	33637.74742	323.00327
10	425	31856.81798	307.9918
15	415	29467.34622	298.00694

5. CONCLUSION

Reducing the size of a metallic material to the nanoscale leads to major changes in its optical response as compared with the bulk metal. The optical properties of palladium (Pd) nanoparticles are extremely important in nanotechnology applications. They are dominated by Localized Surface Plasmon Resonance phenomenon. The characteristics of LSPR (spectral position, amplitude and width) depend on the intrinsic properties of nanoparticles: the size, shape, structure and their environment. The absorption, scattering and extinction cross-sections are calculated using Finite Element Method (FEM) implemented in COMSOL Multiphysics. This work aimed to investigate the size and shape effect on the LSPR of Pd nanoparticles. We have investigated a nanoparticle having the shape of a parallelepiped in two different cases. The first case studied the size effect on the LSPR upon changing the length and width while fixing the height. The second case studied the shape effect on the LSPR upon changing the corners shape. It has been intended to round the corner of the parallelepiped nanoparticle with different radii. In the first case, upon varying the length and width of a parallelepiped palladium nanoparticle, the incident electromagnetic wave was polarized parallel to the x-axis. The peak resonance was red shifted. It reached the visible range when the length and width reached the value of 80nm. We concluded that as the size of the parallelepiped Pd nanoparticle increases, the extinction magnitude enhances whereas the spectral peak position of LSPR is red shifted. The mechanism of the second case was rounding the corners of the parallelepiped with radii from 0nm to 15nm. When the polarization of light is along the x-axis, the peak resonances, which are in the ultraviolet range, decreased with the increase of the radius of the corner. Whereas, when the polarization is along the y-axis, the peak resonances are located in the visible range with blue shifting peak resonance when increasing the radii corners from 0 to 15 nm. Thus, we can deduce the LSPR of a Pd nanoparticles not only affected by the size of the nanoparticle but also by its shape. Keeping in mind that all these parameters which are affecting the LSPR of Pd nanoparticle produced a large enhancement of the electromagnetic field at their surfaces which leads to a wide range of nowadays applications.

REFERENCES

- Adams, C. P., Walker, K. A., Obare, S. O., and Docherty, K. M. (2014). Size-dependent antimicrobial effects of novel palladium nanoparticles. *PLoS ONE* (9), 85–98.
- Amendola, V., Bakr, O. M., & Stellacci, F. (2010). A study of the surface plasmon resonance of silver nanoparticles by the discrete dipole approximation method: effect of shape, size, structure, and assembly. *Plasmonics*, *5*(1), 85-97.
- Baida, H., Billaud, P., Marhaba, S., Christofilos, D., Cottancin, E., Crut, A., & Liz-Marzán, L. M. (2009). Quantitative determination of the size dependence of surface plasmon resonance damping in single Ag@ SiO2 nanoparticles. *Nano letters*, *9*(10), 3463-3469.
- Billaud, P., Marhaba, S., Cottancin, E., Arnaud, L., Bachelier, G., Bonnet, C. & Pellarin, M. (2008). Correlation between the extinction spectrum of a single metal nanoparticle and its electron microscopy image. *The Journal of Physical Chemistry C*, *112*(4), 978-982.
- Bohren, C. F., & Huffman, D. R. (1983). Absorption and scattering of light by small particles. *John Wiley & Sons*.
- Chatterjee, K., Sarkar, S., Rao, K. J. & Paria, S. (2014). Core/shell nanoparticles in biomedical applications. *Advances in colloid and interface science*, *209*, 8-39.

- Chen A, Ostrom C. (2015) Palladium-based nanomaterials: synthesis and electrochemical applications. *Chem Rev.* (115), 11999-2044.
- Chen M, Wu B, Yang J, Zheng N. (2012) Small adsorbate-assisted shape control of Pd and Pt nanocrystals. *Adv Mater.* (24), 862-79.
- Chen X, Shi S, Wei J, Chen M, Zheng N. (2017). Two-dimensional Pd-based nanomaterials for bioapplications. *Sci Bull (Beijing).* (62), 579-88.
- Deplanche, K., Bennett, J. Mikheenko, J. O., Wells, A., Meadows, R., Wood, J. & Macaskie, L. (2014). Catalytic activity of biomass-supported Pd nanoparticles: influence of the biological component in catalytic efficacy and potential application in 'green' synthesis of fine chemicals and pharmaceuticals. *Applied Catalysis B: Environmental*, *147*, 651-665.
- Dickinson, E. J. F., Ekstrom, H. & Fontes, E. (2014). COMSOL Multiphysics: Finite element software for electrochemical analysis. *Electrochemistry Communications, 40*, 71-74.
- El Samad, S. & Marhaba, S. (2022). How Light Polarizations Affect the Localized Surface Plasmon Resonance of Asymmetric Palladium Nanostructures. *Nano, 17*(07), 2250051.
- Fano, U. (1941). The theory of anomalous diffraction gratings and of quasi-stationary waves on metallic surfaces (Sommerfeld's waves). *Optical Society of America, 31*, 213–222.
- Gracia-Pinilla, M. A., Pérez-Tijerina, E., Antúnez-García, J., Fernández-Navarro, C., Tlahuice-Flores, A., Mejia-Rosales, S. & José-Yacamán, M. (2008). On the structure and properties of silver nanoparticles. *The Journal of Physical Chemistry C, 112*(35), 13492-13498.
- Grand, J. & Le Ru1, E.C. (2019). Practical Implementation of Accurate Finite-Element Calculations for Electromagnetic Scattering by Nanoparticles. *Springer, 15*, 109-121.
- Johnson, P. B., & Christy, R. W. (1972). Optical constants of the noble metals. *Physical review B, 6*(12), 4370.
- Kreibig, U., & Vollmer, M. (1995). Optical properties of metal clusters (Vol. 25*). Springer Science & Business Media*.
- Kang, S., Shin, W., Kang, K., Choi, M., Kim, Y., Min, D. & Jamg, H. (2018). Revisiting of Pd nanoparticles in cancer treatment: all-round excellence of porous Pd nanoplates in gene-thermo combinational therapy. *ACS applied materials & interfaces, 10* (16), 13819-13828.
- Kretschmann, E., Raether, H. & Naturforsch, Z. (1968). Radiative decay of non-radiative surface plasmons excited by light. *De Gruyter, 23A*, 2135–2136.
- Lermé, J., Bonnet, C., Broyer, M., Cottancin E., Marhaba, S. & Pellarin, M. (2008). Optical response of metal or dielectric nano-objects in strongly convergent light beams. *Physical Review B, 77*(24), 245406.
- Lermé, J., Bachelier, G., Billaud, P., Bonnet, C., Broyer, M., Cottancin, E. & Pellarin, M. (2008). Optical response of a single spherical particle in a tightly focused light beam: application to the spatial modulation spectroscopy technique. *JOSA A, 25*(2), 493-514.
- Liedberg, B., Nylander, C. & Lundstrom, I. (1983). Surface plasmon resonance for gas detection and biosensing. *Elsevier, Sensors and Actuators, 4*, 299–304.
- Liu Y., Wang D-D., Zhao L., Lin M., Sun H-Z., Sun H-C. *et al*. (2016). Polypyrrole-coated flower-like Pd nanoparticles (Pd NPs@PPy) with enhanced stability and heat conversion efficiency for cancer photothermal therapy. *RSC Adv.* (6), 15854-60
- Marhaba, S., Bachelier, G., Bonnet, C., Broyer, M., Cottancin, E., Grillet, N. & Pellarin, M. (2009). Surface plasmon resonance of single gold nanodimers near the conductive contact limit. *The Journal of Physical Chemistry C, 113*(11), 4349-4356.
- Marhaba, S. (2015). Gold nanoparticle arrays spectroscopy: Observation of electrostatic and radiative dipole interactions. *Nano, 10*(01), 1550007.
- Marhaba, S. (2017). Effect of Size, Shape and Environment on the Optical Response of Metallic Nanoparticles. *IntechOpen*.
- Marhaba, S. & El Samad, S. (2020). Plasmonic coupling of one-dimensional palladium nanoparticle Chains. Nano, *15*(05), 2050060.
- Marhaba, S. & El Samad, S. (2021). Interparticle Distance Effect on the Optical Response of Platinum Dimer Nanoparticles. *Chemistry Africa 4* (2), 477-482.
- Maiti, G., Kayal, U., Karmakar, R., Bhattacharya R.N. (2012). An unexpected rearrangement-hydration reaction sequence of 2*H*-chromenes to dihydrochalcones under catalysis of $HAuCl_4$. *Tetrahedron Lett*, 53, 6321–6325.

- Nehl, C. L., Liao, H., & Hafner, J. H. (2006). Optical properties of star-shaped gold nanoparticles. *Nano letters*, *6*(4), 683-688.
- Otto A. (1968). Physik Z. Excitation of surface plasma waves in silver by the method of frustrated total reflection. *Zeitschrift für Physik A Hadrons and Nucle*, *216*, 398-410.
- Petryayeva, E. & Krull, U. J. (2011). Localized surface plasmon resonance: Nanostructures, bioassays and biosensing-A review. *Analytica Chimica Acta*, *706*(1), 8-24.
- Pradhan, K. & Chakraverty, S. (2018). Finite Element Method In Computational Structural Mechanics. *ScienceDirect*.
- Sachse, A., Linares, N., Barbaro, P., Fajula, F., and Galarneau, A. (2013). Selective hydrogenation over Pd nanoparticles supported on a pore-flow-through silica monolith microreactor with hierarchical porosity. *Dalton Trans*. 42, 1378–1384.
- Sadiku, M.N.O. (2000). Numerical Techniques in Electromagnetics, *CRC Press*.
- Saldan, J., Semenyuk, Y., Marchuk, I. & Reshetnyak, O. (2015). Chemical synthesis and application of palladium nanoparticles. *Journal of Materials Science*, *50*, 2337–2354.
- Wood, R. (1902). On a remarkable case of uneven distribution of light in a diffraction grating spectrum. *Philosophical Magazine*, *18*, 269.
- Yurkina, M.A. & Hoekstraa, A.G. (2007). The discrete dipole approximation: An overview and recent developments. *Journal of Quantitative Spectroscopy & Radiative Transfer*, *106*, 558–589.